Electronic Supporting Information

Improving the photocatalytic H_2 evolution activity of Keggin polyoxometalates anchoring copper-azole complexes†

Qingbo Shen,[ab] Carlos J. Gómez-García,[c] Wenlong Sun,[ab] Xiaoyong Lai[d], Haijun Pang*[a] and Huiyuan Ma*[a]

Section 1 Experimental

Section 2 Supplementary Experimental Characterizations

8. **Figure S8.** Solid state UV-Vis absorption spectra of compound **1**, compound **2** and GeW_{12} polyanion.

9. **Table S1.** Photocatalytic H_2 production conditions for compounds **1** and **2**.

10. **Figure S9.** Optical images: (a) Suspension of compound **1** before irradiation. (b) Heterpolyblue (HPB) suspension of compound **1** after irradiation (Xe lamp off); (c) HPB suspension of compound **1** under irradiation (Xe lamp on); (d) Suspension of compound **1** after exposure to O_2.

11. **Figure S10**. Solution UV-Vis absorption spectrum of the HPB state of compound **1** after exposure to a continuous flow of O_2.

12. **Figure S11**. Comparison of the photocatalytic H_2 evolution rates of 5 hours for compound **1** for different water:acetone ratios.

13. **Figure S12**. Comparison of the photocatalytic H_2 evolution rates of 5 hours for compound **1** for different sacrificial reagents.

14. **Figure S13**. Comparison of the photocatalytic H_2 evolution rates of 5 hours for compound **1** for different methanol concentrations.

15. **Figure S14**. Comparison of the photocatalytic H_2 evolution rates of 5 hours for compound **2** for different water:acetone ratios.

16. **Figure S15**. Comparison of the photocatalytic H_2 evolution rates of 5 hours for compound **2** for different sacrificial reagents.

17. **Figure S16**. Comparison of the photocatalytic H_2 evolution rates of 5 hours for compound **2** for different methanol concentrations.

18. **Figure S17**. Liquid state UV-Vis absorption spectrum of HPB state of compound **2** under Xe irradiation with 300-400nm wavelength; irradiation time: 0, 1, 3, 5, 7, 9, 11min.

19. **Figure S18**. Comparison of the transient photocurrent responses for compound **1** and the physical mixture of GeW_{12} + $CuCl_2$ + 2-ptz.

20. **Figure S19**. Photoluminescence spectra of compounds **1** and **2** with the excitation wavelength at 300 nm.

21. **Figure S20**. Time evolution of the photocatalytic H_2 production for compound **2**.

22. **Figure S21**. High-resolution XPS spectrum of the W(4f) and Cu(2p) region for compounds **1** and **2** after photocatalysis.

23. **Figure S22**. CV curve of compound **2** in a 0.5 M H_2SO_4 solution (pH = 0.28) with a scan rate of 0.1 V s^{-1}.

24. **Figure S23**. (a) HPBs state of compound **1** solution under Xe light (λ > 350 nm). (b) HPBs state of compound **1** solution after irradiation with λ > 400 nm.

25. **Figure S24**. Solution UV-Vis absorption spectrum of the HPB state of compound **2** after exposure to a continuous flow of O_2.

26. **Figure S25**. CV curve of GeW_{12} precursor in a 0.5 M H_2SO_4 solution (pH = 0.28) with a scan rate of 0.1 V s^{-1}. (*vs.* Ag/AgCl)

Section 3 Supplementary Discussion

1. The photocatalytic mechanism for GeW_{12} (without copper)

Section 4 References

Section 1 Experimental Section

1. Materials and General Methods

All reagents are commercially available and were used as received without further purification. C, H and N elemental analyses were performed on a Perkin-Elmer 2400 CHN elemental analyser and for Ge, W and Cu on a Leaman inductively coupled plasma (ICP) spectrometer. The Fourier transform infrared (FT-IR) spectrum was recorded with KBr pellets in the range 4000-400 cm^{-1} with a Nicolet AVATAR FT-IR360 spectrometer. The powder X-ray diffraction (PXRD) data were collected on a Rigaku RINT2000 diffractometer at room temperature. Optical properties were also studied by diffuse reflectance UV-vis spectroscopy (Lambda 35 spectrometer). Liquid UV-vis spectra were performed on a TU-1900 spectrophotometer. W and Cu elements valence were analysed on an X-ray photoelectron spectroscopy spectrometer. A CHI660 electrochemical workstation was used for the cyclic voltammetry measurements (CV), photocurrent-time (I-T) and impedance spectra (EIS). A conventional three-electrode system was used, with glassy carbon (GCE) and ITO glass electrodes as working electrodes, a commercial Ag/AgCl as reference electrode and a platinum wire as counter electrode. The electrochemical CV curves were carried out in 0.5 M H_2SO_4 solution at the scan rate of 0.1 V s^{-1}. The photocurrent-time measurements were carried out in 0.25 M Na_2SO_4 solution. A 500 W Xenon lamp (λ > 350 nm) was used as the light source during the measurements. Electrochemical impedance spectroscopy (EIS) tests were conducted in the frequency range 0.1 Hz to 100 kHz.

The potentials *vs.* NHE are calculated according to the equation below:[1]

$E_{NHE} = E_{Ag/AgCl} + 0.059\ pH + E^{\theta}_{Ag/AgCl}$ (NHE at pH = 0).

For converting the obtained reduction potential (*vs.* Ag/AgCl) of compound **1** to RHE (NHE at pH = 0)

I', E_{NHE} = -0.529 V + 0.209 V = -0.320 V

II', E_{NHE} = -0.383 V + 0.209 V = -0.174 V

III', E_{NHE} = -0.189 V + 0.209 V = +0.020 V

IV', E_{NHE} = +0.124 V + 0.209 V = +0.333 V

Therefore, the four reduction peak potentials of compound **1** are -0.320 V (I'), -0.174 V (II'), +0.020 V (III') and +0.333 V (IV') (*vs.* NHE), respectively.

We convert the reduction potential (*vs.* Ag/AgCl) of compound **2** to RHE (NHE at pH = 0).

I', E_{NHE} = -0.560 V + 0.209 V = -0.351 V

II', E_{NHE} = -0.402 V + 0.209 V = -0.193 V

III', E_{NHE} = -0.248 V + 0.209 V = -0.039 V

IV', E_{NHE} = +0.043 V + 0.209 V = +0.252 V

V', E_{NHE} = +0.480 V + 0.209 V = +0.689 V

Therefore, the five reduction peak potentials of compound **2** are -0.351 V (I'), -0.193 V (II'), -0.039 (III'), +0.252 V (IV') and +0.689 V (V') (*vs.* NHE), respectively.

2. Preparation of the Modified Electrodes

ITO glass electrode: The as-synthesized samples (2 mg) were ground and dispersed into a mixture of 1 mL of ethanol and 10 μL of Nafion. The working electrodes were prepared by drop casting 10 μL of this suspension onto an ITO glass substrate electrode surface (1 cm^2) and dried at room temperature. (Used for photocurrent-time measurement).

Glassy carbon electrode (GCE): Prior to be modified, the GCE was polished carefully with 0.05 μm alumina powders and then cleaned with ethanol and deionized water. First 3 mg of the as-synthesized samples were ground during 30 min, and then 3 mg of carbon black (Vulcan XC-72R) were added to the above ground samples and the mixture was grounded for another 30 min.

Catalyst inks were prepared by adding 2 mg of the prepared catalyst powders into a mixture of water/ethanol = (750/250 μL) with 0.5 wt % Nafion (50 μL) and the suspension was ultrasonicated for 30 min. This suspension (5 μL) was transferred onto the washed GCE and dried in air at room temperature before electrochemical

experiments. (Used for cyclic voltammetry and impedance spectra measurements).

3. Synthesis of compounds 1 and 2

$[Cu^{II}_5(2\text{-ptza})_6(H_2O)_4(GeW_{12}O_{40})]\cdot 4H_2O$ (1). A mixture of $K_4[GeW_{12}O_{40}]$ (0.03 g, 0.095mmol), $CuCl_2\cdot 2H_2O$ (0.167 g, 0.98 mmol), 2-pzta (0.04 g, 0.272 mmol) and water (40 mL) was stirred for 2 h. The resulting solution was transferred to a Teflon lined autoclave and kept under autogenous pressure at 160 ºC for 3 days with pH = 2.0 adjusted with 0.5 M HCl. After slow cooling to room temperature at a rate of 10 °C /h, blue block crystals of **1** were filtered, washed with distilled water and dried at room temperature (Yield, 65 %, based on W). Anal. Calcd. for $GeW_{12}O_{48}Cu_5H_{40}N_{30}C_{36}$: Ge, 1.706; W, 51.82; Cu, 7.463; H, 0.947; N, 9.87; C, 10.16 (%). Found: Ge, 1.783; W, 50.96; Cu, 7.561; H, 0.822; N, 9.92; C, 9.68 (%).

$[Cu^{I}_2(ppz)_4][H_2GeW_{12}O_{40}]\cdot 8H_2O$ (2). Compound **2** was prepared by the above method except that the 2-pzta ligand was replaced by ppz (0.04 g, 0.27 mmol). After slow cooling to room temperature at a rate of 10 °C /h, dark red block crystals were filtered, washed with distilled water and dried at room temperature (Yield, 62 %, based on W). Anal. Calcd. for $Cu_2N_{12}C_{32}GeW_{12}O_{48}H_{46}$: Cu, 3.369; N, 4.455; C, 10.19; Ge, 1.926; W, 58.48; H, 1.229; Found: Cu, 3.472; N, 4.365; C, 11.23; Ge, 1.849; W, 59.68; H, 1.343.

4. X-ray Crystallography

Single crystal X-ray diffraction data collection for compounds **1** and **2** were performed using a Bruker Smart Apex CCD diffractometer with Mo-K*a* radiation at 296 K. Multi-scan absorption corrections were applied. The two structures were solved by Direct Methods and refined by full-matrix least-squares on F^2 using the SHELXTL 97 crystallographic software package. Anisotropic displacement parameters were used to refine all non-hydrogen atoms. The organic hydrogen atoms were generated geometrically. All H atoms on C atoms were fixed at the calculated positions. The H atoms of the water molecules in **1** and **2** cannot be found from the

residual peaks and were directly included in the final molecular formula.

5. General process for photocatalytic hydrogen evolution

Photocatalytic hydrogen evolution experiments were performed in a quartz reaction vessel under a 500 W Xe lamp in 20 mL of a 1:2 mixture of H_2O/acetone solution containing 20 % methanol (v/v) as electron sacrificial agent. The as-synthesized samples (5 mg) were used as photosensitizers and photocatalysts without co-catalysts. To remove the air inside and make sure that the reaction system was under anaerobic conditions, the reaction vessel was purged/evacuated with N_2 for at least 5 min before irradiation. The reaction solution was stirred continuously and cooled to 5 °C. The generated H_2 was characterized by GC 7890T instrument analysis using a 5 Å molecular sieve column (0.6 m × 3 mm), thermal conductivity detector, and N_2 as carrier gas.

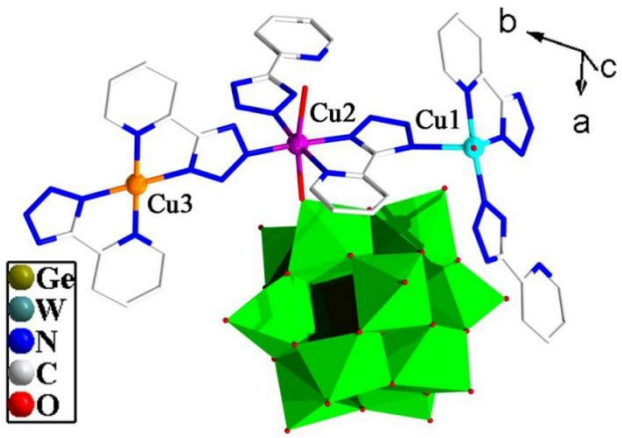

Figure S1. View of the asymmetric unit of **1**. All hydrogen atoms and free water molecules are omitted for clarity.

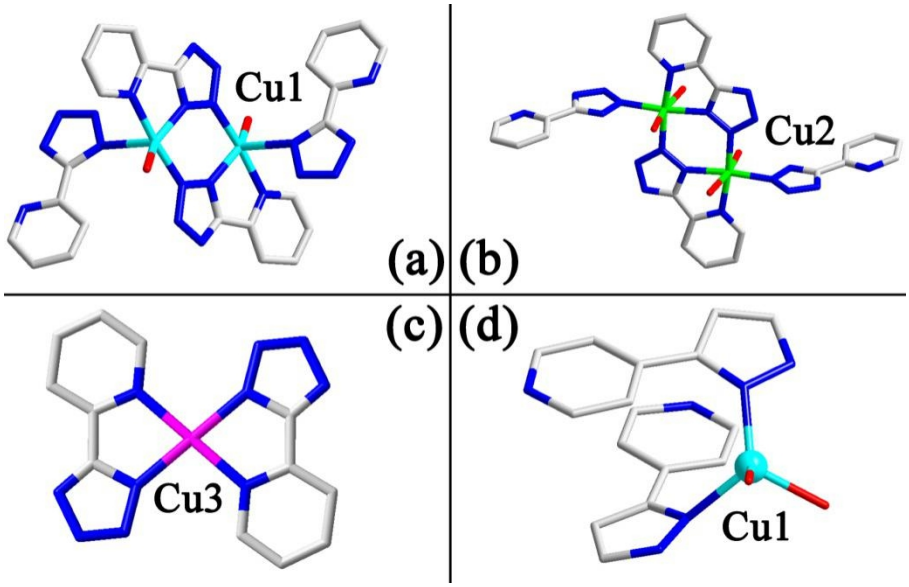

Figure S2. View of the structures of the Cu-azole complexes: a-c for compound **1** and d for compound **2**.

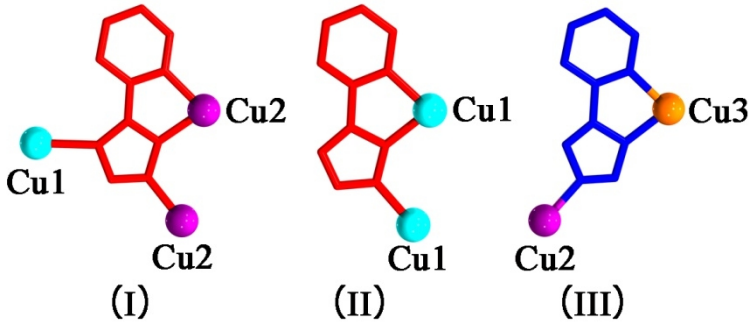

Figure S3. View of the three coordination modes of the deprotonated 2-ptz$^-$ ligands in compound **1**.

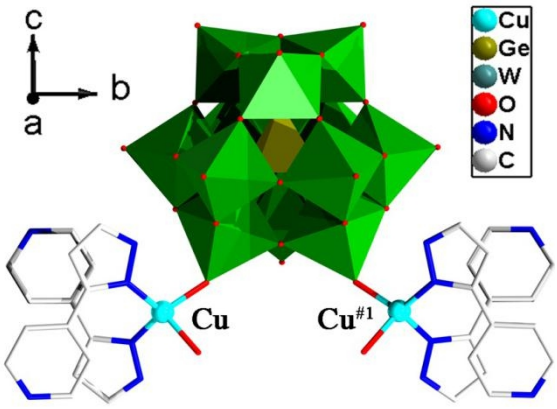

Figure S4. View of the structure of **2**. All hydrogen atoms and crystallization water molecules are omitted for clarity. (Symmetry codes: #1: x, 1-y, z)

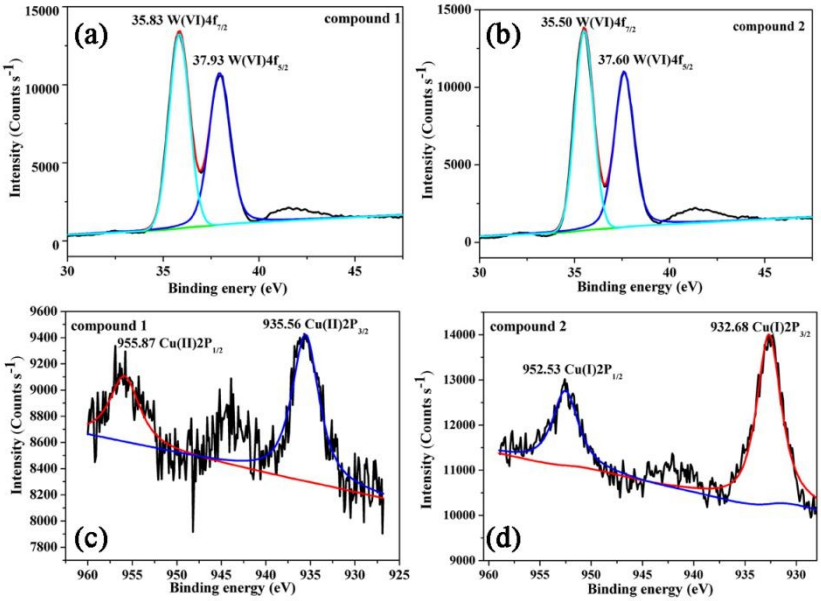

Figure S5. High-resolution XPS spectra of the Cu(2p) and W(4f) region for compounds **1** and **2**， before photocatalysis.

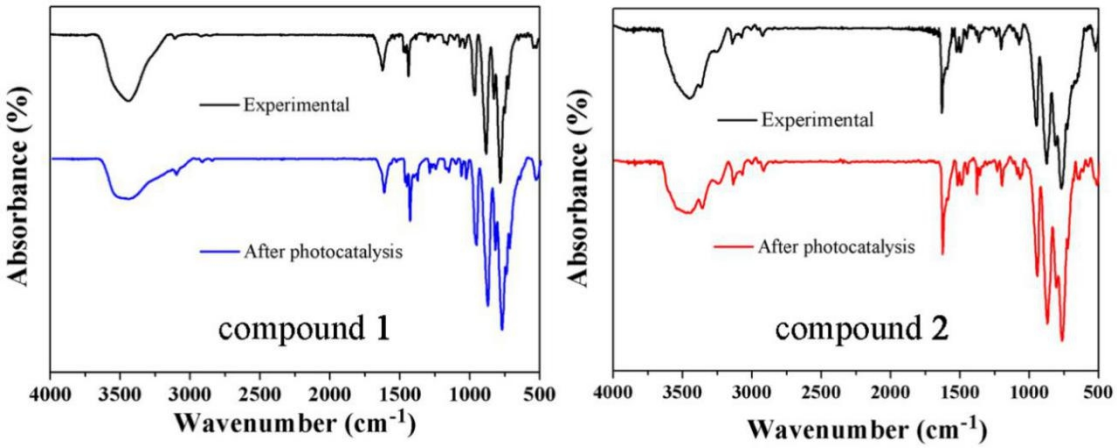

Figure S6. Experimental IR spectra of compounds **1** and **2** before (black lines) and after (blue and red lines) photocatalysis.

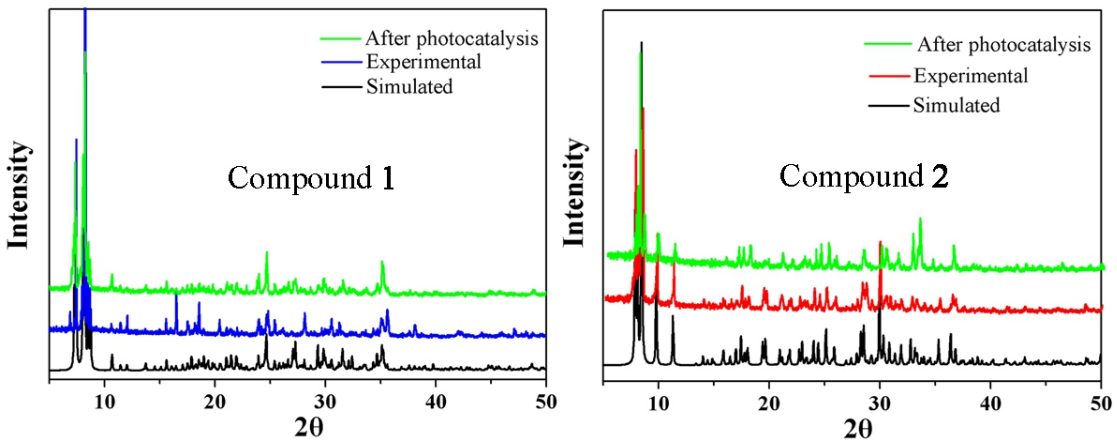

Figure S7. Simulated (black) PXRD diffractograms before (blue and red) and after (green) photocatalysis for compounds **1** and **2**.

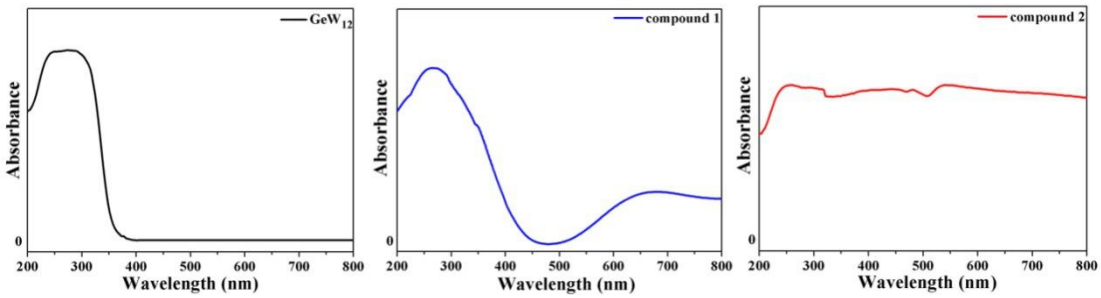

Figure S8. Solid state UV-Vis absorption spectra of GeW_{12} polyanion (black line), compound **1** (blue line), and compound **2** (red line).

Table S1. Photocatalytic H_2 production conditions for compounds **1** and **2**.

Catalyst	Amount	Light (λ/nm)	Electron donor	H_2 production rate
Compound **1**[a]	5 mg	No	CH_3OH	No
Compound **1**[a]	no	350-780	CH_3OH	No
Compound **1**[a]	5 mg	350-780	No	No
Compound **1**[a]	5 mg	350-780	CH_3OH	3.81 mmol g^{-1} h^{-1}
Compound **1**[b]	5 mg	350-780	CH_3OH	0.17 mmol g^{-1} h^{-1}
Compound **1**[c]	5 mg	350-780	CH_3OH	0.73 mmol g^{-1} h^{-1}
Compound **1**[d]	5 mg	350-780	CH_3OH	0.46 mmol g^{-1} h^{-1}
Compound **1**[e]	5 mg	350-780	CH_3OH	1.02 mmol g^{-1} h^{-1}
Compound **2**[a]	5 mg	400-780	CH_3OH	Trace
(ppz+GeW_{12})[a]	5 mg	400-780	CH_3OH	No
(2-ptza+GeW_{12})[a]	5 mg	400-780	CH_3OH	No
Compound **1**[a]	5 mg	400-780	CH_3OH	No
Compound **1**[a]	5 mg	350-400	CH_3OH	Trace

Reaction conditions: (a) 20 mL of a 1:2 mixture of H_2O/acetone solution containing 20 % methanol (v/v) as electron sacrificial agent. (b) 20 mL of H_2O containing 20 % methanol (v/v) as electron sacrificial agent. (c) 20 mL of a 1:2 mixture of H_2O/DMF solution containing 20 % methanol (v/v) as electron sacrificial agent. (d) 20 mL of a 1:2 mixture of H_2O/ethanol solution containing 20 % methanol (v/v) as electron sacrificial agent. (e) 20 mL of a 1:2 mixture of H_2O/acetonitrile solution containing 20 % methanol (v/v) as electron sacrificial agent.

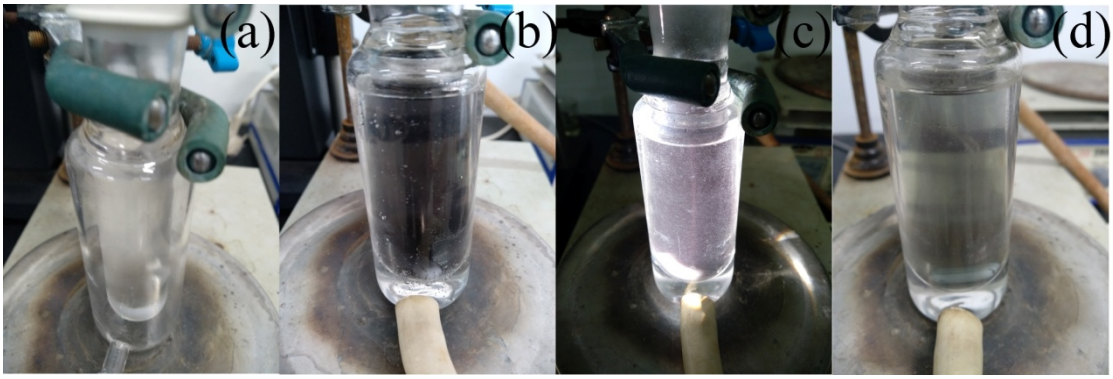

Figure S9. Optical images: (a) Suspension of compound **1** before irradiation. (b) Heterpolyblue (HPB) suspension of compound **1** after irradiation (Xe lamp off); (c) HPB suspension of compound **1** under irradiation (Xe lamp on); (d) Suspension of compound **1** after exposure to O_2.

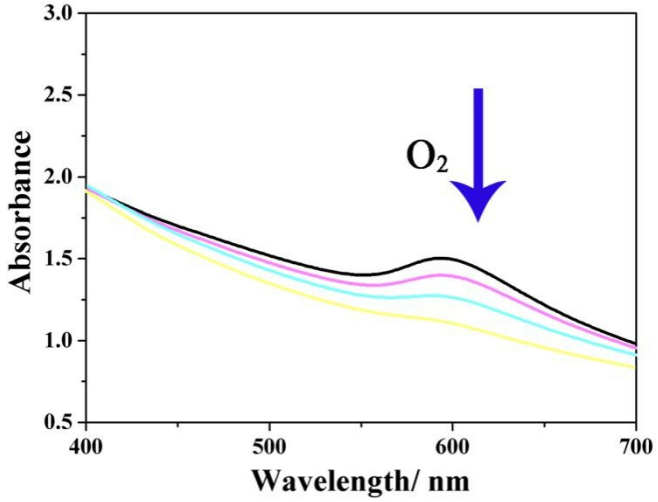

Figure S10. Solution UV-Vis absorption spectrum of the HPB state of compound **1** after exposure to a continuous flow of O_2.

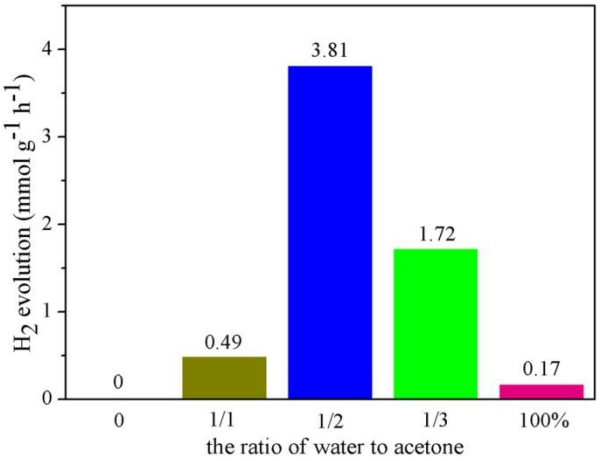

Figure S11. Comparison of the photocatalytic H_2 evolution rates of 5 hours for

compound **1** for different water:acetone ratios.

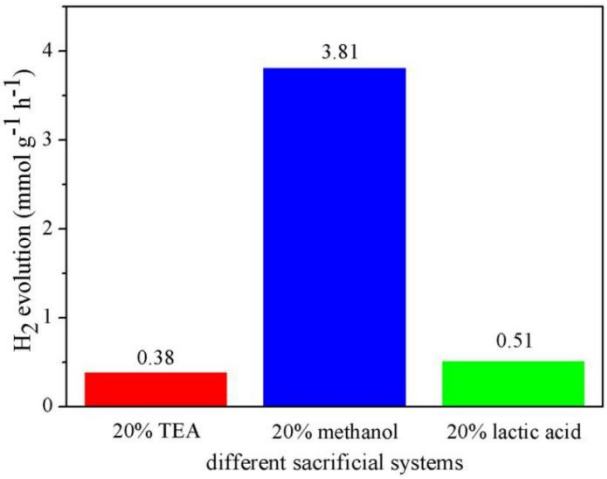

Figure S12. Comparison of the photocatalytic H_2 evolution rates of 5 hours for compound **1** for different sacrificial reagents.

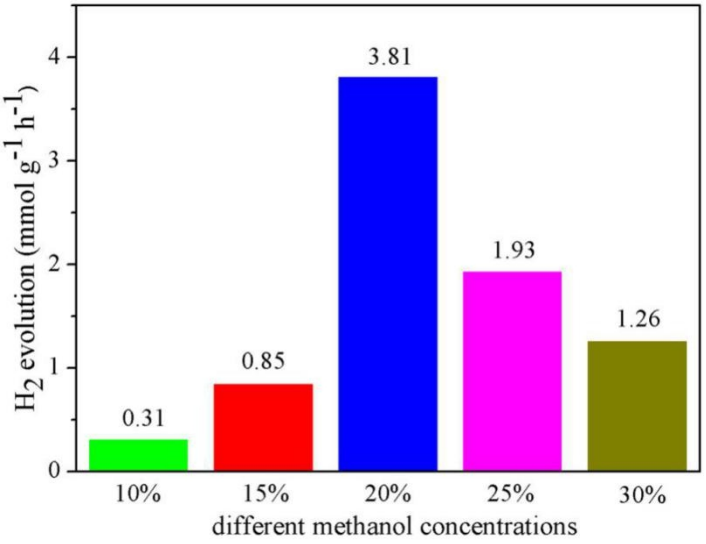

Figure S13. Comparison of the photocatalytic H_2 evolution rates of 5 hours for compound **1** for different methanol concentrations.

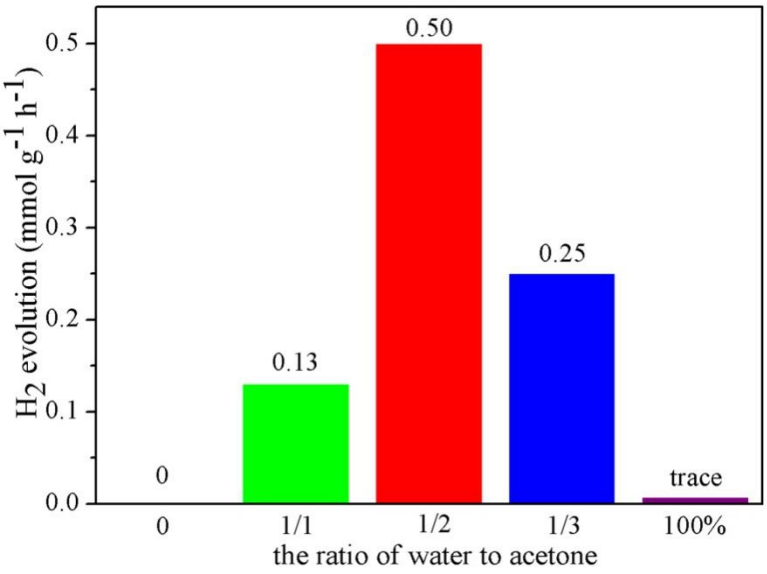

Figure S14. Comparison of the photocatalytic H_2 evolution rates of 5 hours for compound **2** for different water:acetone ratios.

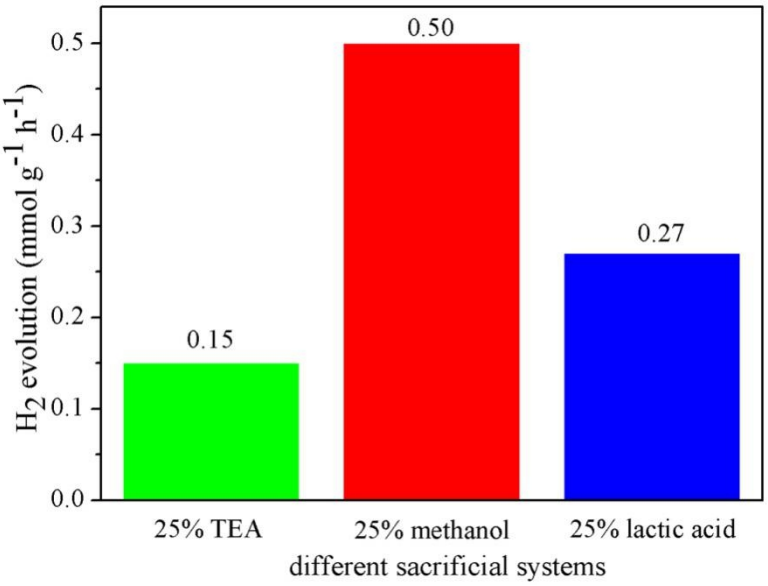

Figure S15. Comparison of the photocatalytic H_2 evolution rates of 5 hours for compound **2** for different sacrificial reagents.

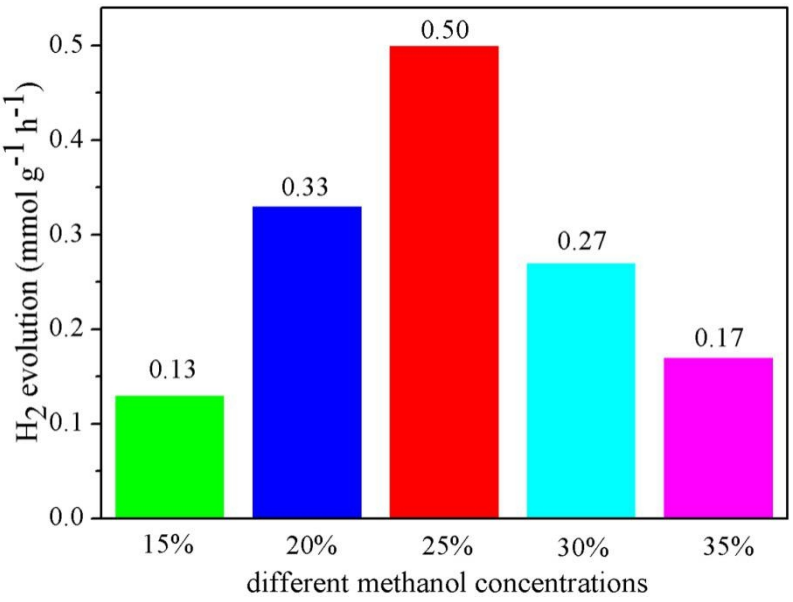

Figure S16. Comparison of the photocatalytic H_2 evolution rates of 5 hours for compound **2** for different methanol concentrations.

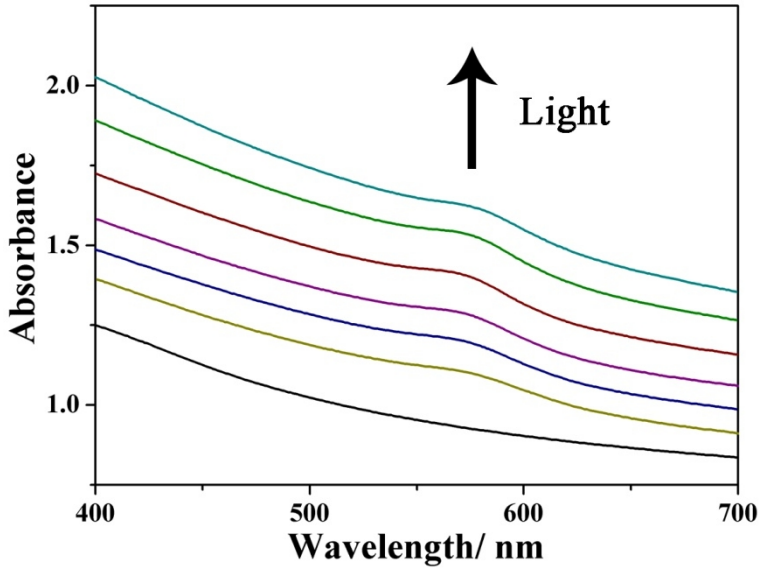

Figure S17. Liquid state UV-Vis absorption spectrum of HPB state of compound **2** under Xe irradiation with 300-400nm wavelength; irradiation time: 0, 1, 3, 5, 7, 9, 11min.

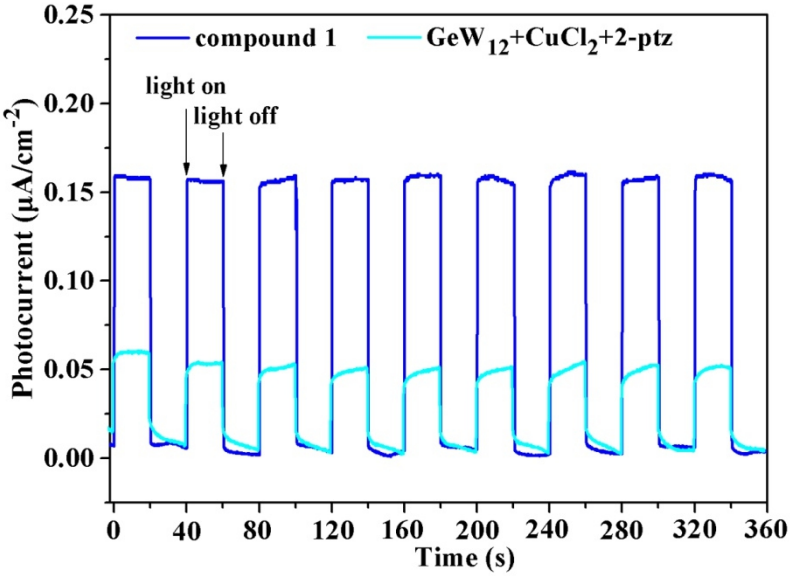

Figure S18. Comparison transient photocurrent responses for compound **1** and the physical mixture of GeW_{12} + $CuCl_2$ + 2-ptz.

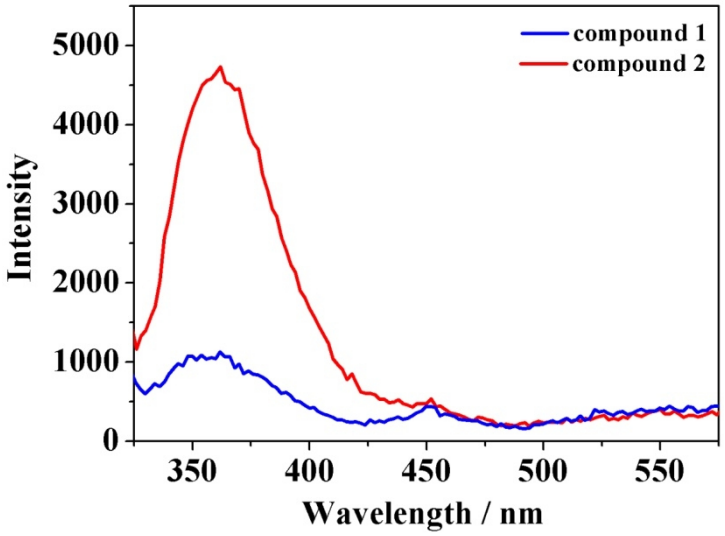

Figure S19. Photoluminescence spectra of compounds **1** and **2** with the excitation wavelength at 300 nm.

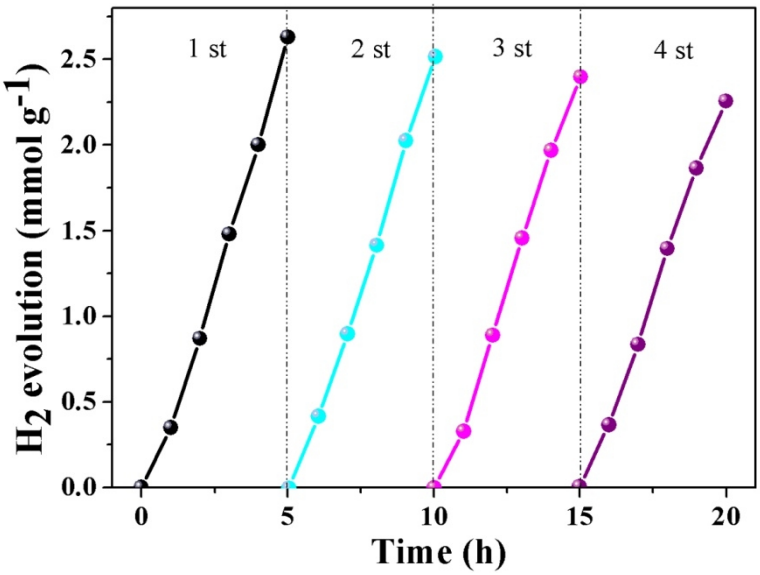

Figure S20. Time evolution of the photocatalytic H_2 production for compound **2**.

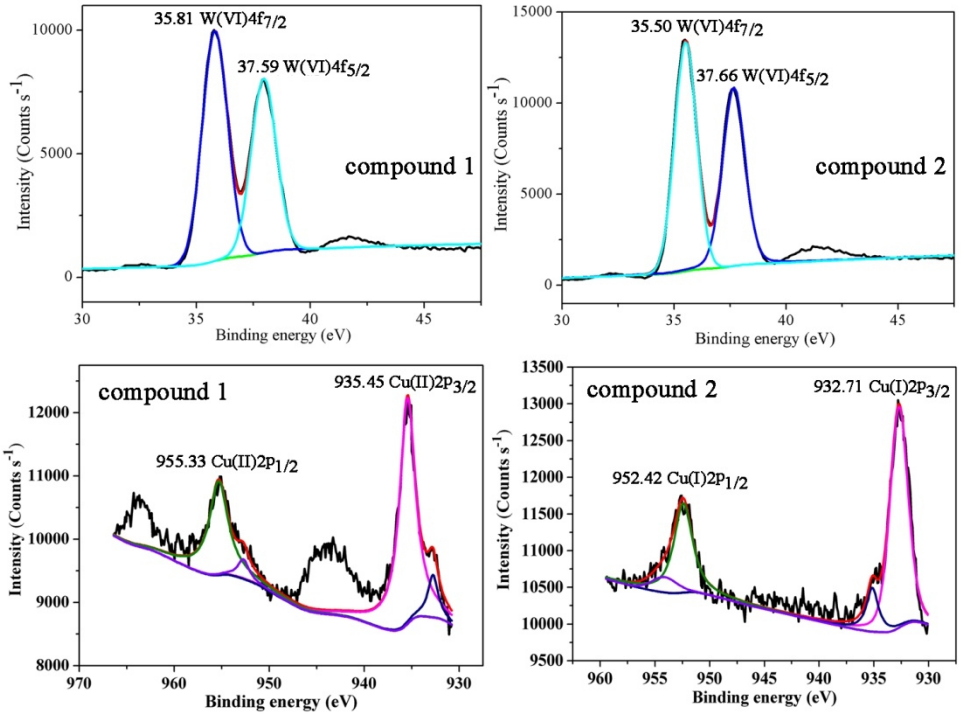

Figure S21. High-resolution XPS spectrum of the W(4f) and Cu(2p) region for compounds **1** and **2** after photocatalysis.

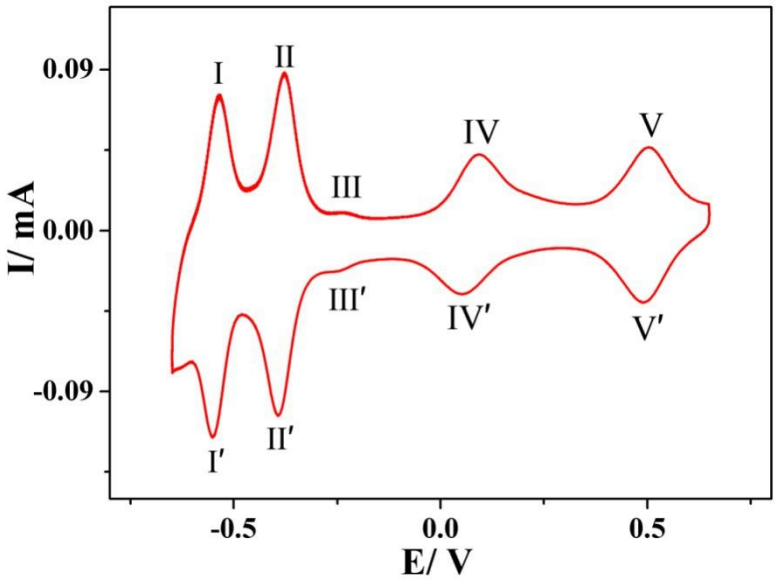

Figure S22. CV curve of compound **2** in a 0.5 M H_2SO_4 solution (pH = 0.28) with a scan rate of 0.1 V s^{-1}. (*vs.* Ag/AgCl)

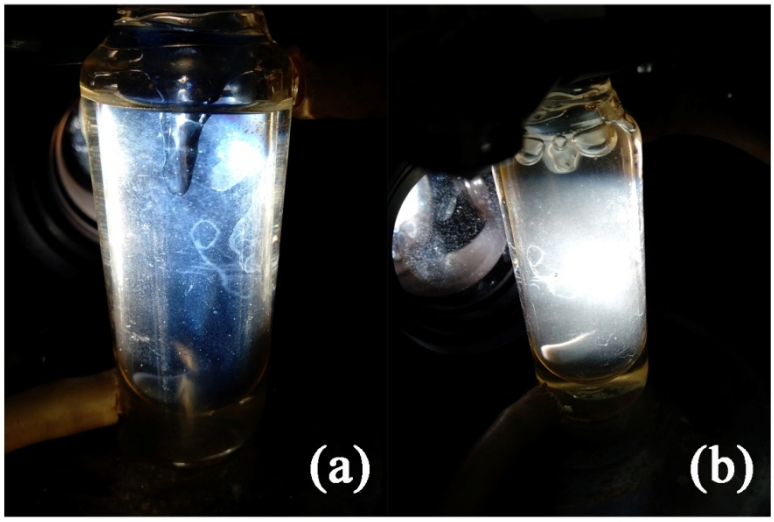

Figure S23. (a) HPBs state of compound **1** solution under Xe light (λ > 350 nm). (b) HPBs state of compound **1** solution after irradiation with λ > 400 nm.

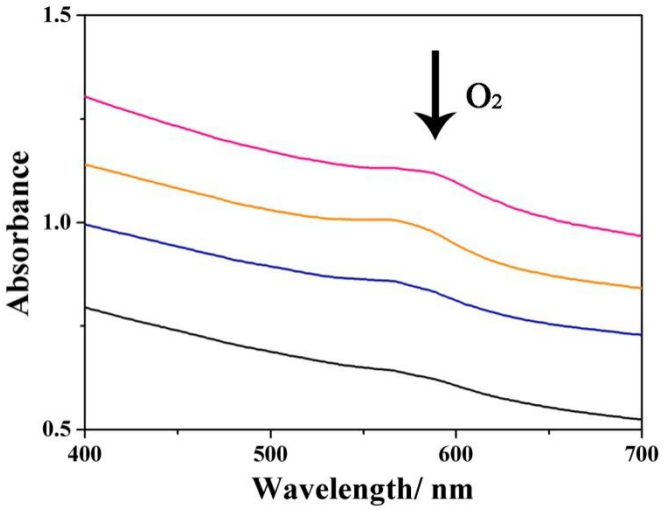

Figure S24. Solution UV-Vis absorption spectrum of the HPB state of compound **2** after exposure to a continuous flow of O_2.

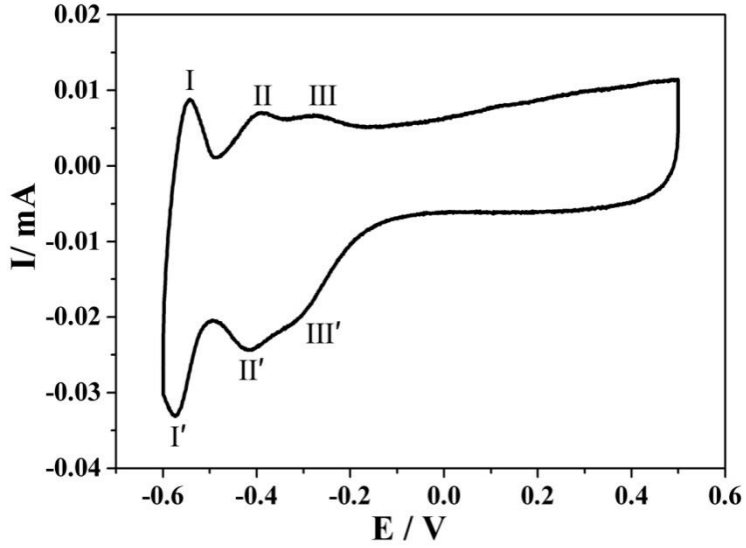

Figure S25. CV curve of GeW_{12} precursor in a 0.5 M H_2SO_4 solution (pH = 0.28) with a scan rate of 0.1 V s^{-1}. (*vs.* Ag/AgCl)

Section 3 Supplementary Discussion

The photocatalytic mechanism for GeW_{12} (without copper)

As a photosensitizer, GeW_{12} polyanions can also act as photocatalysis to produce hydrogen due to its reduction potential meeting the conditions for hydrogen evolution from reducing water. The CV curve of GeW_{12} in a 0.5 M H_2SO_4 solution at a scan rate of 0.1 V s^{-1} is presented in Fig. S25. The GeW_{12} shows three pairs of redox peaks (I-I',

II-II' and III-III') with the reduction potentials at -0.574 V (I'), -0.415 V (II') and -0.300 V (III') (*vs.* Ag/AgCl). According to the formula, $E_{RHE} = E_{AgCl} + 0.059\ pH + E_{AgCl}^{\theta}$, E_{AgCl}^{θ} (3.0 M NaCl) = 0.209 V at 25℃, and we get the corresponding reduction potential are -0.365 V (I'), -0.206 V (II'), and -0.091 V (III') (*vs.* NHE). They are both negative enough (the potential of H^+/H_2 is 0 V vs. NHE) to drive H_2 production. Therefore, GeW_{12} polyanion can also be used as a catalytic site. However, when GeW_{12} is used as catalyst, the photogenerated electrons and holes are not separated effectively, so the photocatalytic hydrogen production efficiency is very low.

Section 4 References

1. S. J. Hong, S. Lee, J. S. Jang and J. S. Lee, *Energy Environ. Sci.*, 2011, **4**, 1781-1788.